Physics Letters B 679 (2009) 321–329

Contents lists available at ScienceDirect

Physics Letters B

www.elsevier.com/locate/physletb

Photoproduction of J/ψ and of high mass e^+e^- in ultra-peripheral Au + Au collisions at $\sqrt{s_{NN}} = 200$ GeV

PHENIX Collaboration

S. Afanasiev [q], C. Aidala [g], N.N. Ajitanand [aq], Y. Akiba [ak,al], J. Alexander [aq], A. Al-Jamel [ag], K. Aoki [w,ak], L. Aphecetche [as], R. Armendariz [ag], S.H. Aronson [c], R. Averbeck [ar], T.C. Awes [ah], B. Azmoun [c], V. Babintsev [n], A. Baldisseri [h], K.N. Barish [d], P.D. Barnes [z], B. Bassalleck [af], S. Bathe [d], S. Batsouli [g], V. Baublis [aj], F. Bauer [d], A. Bazilevsky [c], S. Belikov [c,p,1], R. Bennett [ar], Y. Berdnikov [an], M.T. Bjorndal [g], J.G. Boissevain [z], H. Borel [h], K. Boyle [ar], M.L. Brooks [z], D.S. Brown [ag], D. Bucher [ac], H. Buesching [c], V. Bumazhnov [n], G. Bunce [c,al], J.M. Burward-Hoy [z], S. Butsyk [ar], S. Campbell [ar], J.-S. Chai [r], S. Chernichenko [n], J. Chiba [s], C.Y. Chi [g], M. Chiu [g], I.J. Choi [az], T. Chujo [aw], V. Cianciolo [ah], C.R. Cleven [l], Y. Cobigo [h], B.A. Cole [g], M.P. Comets [ai], Z. Conesa del Valle [x], P. Constantin [p], M. Csanád [j], T. Csörgő [t], T. Dahms [ar], K. Das [k], G. David [c], H. Delagrange [as], A. Denisov [n], D. d'Enterria [g], A. Deshpande [al,ar], E.J. Desmond [c], O. Dietzsch [ao], A. Dion [ar], J.L. Drachenberg [a], O. Drapier [x], A. Drees [ar], A.K. Dubey [ay], A. Durum [n], V. Dzhordzhadze [at], Y.V. Efremenko [ah], J. Egdemir [ar], A. Enokizono [m], H. En'yo [ak,al], B. Espagnon [ai], S. Esumi [av], D.E. Fields [af,al], F. Fleuret [x], S.L. Fokin [v], B. Forestier [aa], Z. Fraenkel [ay,1], J.E. Frantz [g], A. Franz [c], A.D. Frawley [k], Y. Fukao [w,ak], S.-Y. Fung [d], S. Gadrat [aa], F. Gastineau [as], M. Germain [as], A. Glenn [at], M. Gonin [x], J. Gosset [h], Y. Goto [ak,al], R. Granier de Cassagnac [x], N. Grau [p], S.V. Greene [aw], M. Grosse Perdekamp [o,al], T. Gunji [e], H.-Å. Gustafsson [ab], T. Hachiya [m,ak], A. Hadj Henni [as], J.S. Haggerty [c], M.N. Hagiwara [a], H. Hamagaki [e], H. Harada [m], E.P. Hartouni [y], K. Haruna [m], M. Harvey [c], E. Haslum [ab], K. Hasuko [ak], R. Hayano [e], M. Heffner [y], T.K. Hemmick [ar], J.M. Heuser [ak], X. He [l], H. Hiejima [o], J.C. Hill [p], R. Hobbs [af], M. Holmes [aw], W. Holzmann [aq], K. Homma [m], B. Hong [u], T. Horaguchi [ak,au], M.G. Hur [r], T. Ichihara [ak,al], K. Imai [w,ak], M. Inaba [av], D. Isenhower [a], L. Isenhower [a], M. Ishihara [ak], T. Isobe [e], M. Issah [aq], A. Isupov [q], B.V. Jacak [ar,2], J. Jia [g], J. Jin [g], O. Jinnouchi [al], B.M. Johnson [c,*], K.S. Joo [ad], D. Jouan [ai], F. Kajihara [e,ak], S. Kametani [e,ax], N. Kamihara [ak,au], M. Kaneta [al], J.H. Kang [az], T. Kawagishi [av], A.V. Kazantsev [v], S. Kelly [f], A. Khanzadeev [aj], D.J. Kim [az], E. Kim [ap], Y.-S. Kim [r], E. Kinney [f], A. Kiss [j], E. Kistenev [c], A. Kiyomichi [ak], C. Klein-Boesing [ac], L. Kochenda [aj], V. Kochetkov [n], B. Komkov [aj], M. Konno [av], D. Kotchetkov [d], A. Kozlov [ay], P.J. Kroon [c], G.J. Kunde [z], N. Kurihara [e], K. Kurita [am,ak], M.J. Kweon [u], Y. Kwon [az], G.S. Kyle [ag], R. Lacey [aq], J.G. Lajoie [p], A. Lebedev [p], Y. Le Bornec [ai], S. Leckey [ar], D.M. Lee [z], M.K. Lee [az], M.J. Leitch [z], M.A.L. Leite [ao], H. Lim [ap], A. Litvinenko [q], M.X. Liu [z], X.H. Li [d], C.F. Maguire [aw], Y.I. Makdisi [c], A. Malakhov [q], M.D. Malik [af], V.I. Manko [v], H. Masui [av], F. Matathias [ar], M.C. McCain [o], P.L. McGaughey [z], Y. Miake [av], T.E. Miller [aw], A. Milov [ar], S. Mioduszewski [c], G.C. Mishra [l], J.T. Mitchell [c], D.P. Morrison [c], J.M. Moss [z], T.V. Moukhanova [v], D. Mukhopadhyay [aw], J. Murata [am,ak], S. Nagamiya [s], Y. Nagata [av], J.L. Nagle [f], M. Naglis [ay], T. Nakamura [m], J. Newby [y], M. Nguyen [ar], B.E. Norman [z], A.S. Nyanin [v], J. Nystrand [ab], E. O'Brien [c], C.A. Ogilvie [p], H. Ohnishi [ak], I.D. Ojha [aw], H. Okada [w,ak], K. Okada [al], O.O. Omiwade [a], A. Oskarsson [ab], I. Otterlund [ab], K. Ozawa [e], D. Pal [aw], A.P.T. Palounek [z], V. Pantuev [ar], V. Papavassiliou [ag], J. Park [ap], W.J. Park [u], S.F. Pate [ag], H. Pei [p], J.-C. Peng [o], H. Pereira [h], V. Peresedov [q], D.Yu. Peressounko [v], C. Pinkenburg [c], R.P. Pisani [c], M.L. Purschke [c], A.K. Purwar [ar], H. Qu [l], J. Rak [p], I. Ravinovich [ay], K.F. Read [ah,at], M. Reuter [ar], K. Reygers [ac], V. Riabov [aj], Y. Riabov [aj], G. Roche [aa], A. Romana [x,1], M. Rosati [p], S.S.E. Rosendahl [ab], P. Rosnet [aa], P. Rukoyatkin [q], V.L. Rykov [ak], S.S. Ryu [az], B. Sahlmueller [ac], N. Saito [w,ak,al], T. Sakaguchi [e,ax], S. Sakai [av], V. Samsonov [aj], H.D. Sato [w,ak], S. Sato [c,s,av], S. Sawada [s], V. Semenov [n], R. Seto [d], D. Sharma [ay], T.K. Shea [c],

0370-2693/$ – see front matter
doi:10.1016/j.physletb.2009.07.061

I. Shein [n], T.-A. Shibata [ak,au], K. Shigaki [m], M. Shimomura [av], T. Shohjoh [av], K. Shoji [w,ak], A. Sickles [ar], C.L. Silva [ao], D. Silvermyr [ah], K.S. Sim [u], C.P. Singh [b], V. Singh [b], S. Skutnik [p], W.C. Smith [a], A. Soldatov [n], R.A. Soltz [y], W.E. Sondheim [z], S.P. Sorensen [at], I.V. Sourikova [c], F. Staley [h], P.W. Stankus [ah], E. Stenlund [ab], M. Stepanov [ag], A. Ster [t], S.P. Stoll [c], T. Sugitate [m], C. Suire [ai], J.P. Sullivan [z], J. Sziklai [t], T. Tabaru [al], S. Takagi [av], E.M. Takagui [ao], A. Taketani [ak,al], K.H. Tanaka [s], Y. Tanaka [ae], K. Tanida [ak,al], M.J. Tannenbaum [c], A. Taranenko [aq], P. Tarján [i], T.L. Thomas [af], M. Togawa [w,ak], J. Tojo [ak], H. Torii [ak], R.S. Towell [a], V.-N. Tram [x], I. Tserruya [ay], Y. Tsuchimoto [m,ak], S.K. Tuli [b], H. Tydesjö [ab], N. Tyurin [n], C. Vale [p], H. Valle [aw], H.W. van Hecke [z], J. Velkovska [aw], R. Vertesi [i], A.A. Vinogradov [v], E. Vznuzdaev [aj], M. Wagner [w,ak], X.R. Wang [ag], Y. Watanabe [ak,al], J. Wessels [ac], S.N. White [c], N. Willis [ai], D. Winter [g], C.L. Woody [c], M. Wysocki [f], W. Xie [d,al], A. Yanovich [n], S. Yokkaichi [ak,al], G.R. Young [ah], I. Younus [af], I.E. Yushmanov [v], W.A. Zajc [g], O. Zaudtke [ac], C. Zhang [g], J. Zimányi [t,1], L. Zolin [q]

[a] *Abilene Christian University, Abilene, TX 79699, United States*
[b] *Department of Physics, Banaras Hindu University, Varanasi 221005, India*
[c] *Brookhaven National Laboratory, Upton, NY 11973-5000, United States*
[d] *University of California – Riverside, Riverside, CA 92521, United States*
[e] *Center for Nuclear Study, Graduate School of Science, University of Tokyo, 7-3-1 Hongo, Bunkyo, Tokyo 113-0033, Japan*
[f] *University of Colorado, Boulder, CO 80309, United States*
[g] *Columbia University, New York, NY 10027 and Nevis Laboratories, Irvington, NY 10533, United States*
[h] *Dapnia, CEA Saclay, F-91191, Gif-sur-Yvette, France*
[i] *Debrecen University, H-4010 Debrecen, Egyetem tér 1, Hungary*
[j] *ELTE, Eötvös Loránd University, H-1117 Budapest, Pázmány P. s. 1/A, Hungary*
[k] *Florida State University, Tallahassee, FL 32306, United States*
[l] *Georgia State University, Atlanta, GA 30303, United States*
[m] *Hiroshima University, Kagamiyama, Higashi-Hiroshima 739-8526, Japan*
[n] *IHEP Protvino, State Research Center of Russian Federation, Institute for High Energy Physics, Protvino 142281, Russia*
[o] *University of Illinois at Urbana-Champaign, Urbana, IL 61801, United States*
[p] *Iowa State University, Ames, IA 50011, United States*
[q] *Joint Institute for Nuclear Research, 141980 Dubna, Moscow Region, Russia*
[r] *KAERI, Cyclotron Application Laboratory, Seoul, Republic of Korea*
[s] *KEK, High Energy Accelerator Research Organization, Tsukuba, Ibaraki 305-0801, Japan*
[t] *KFKI Research Institute for Particle and Nuclear Physics of the Hungarian Academy of Sciences (MTA KFKI RMKI), H-1525 Budapest 114, PO Box 49, Budapest, Hungary*
[u] *Korea University, Seoul, 136-701, Republic of Korea*
[v] *Russian Research Center "Kurchatov Institute", Moscow, Russia*
[w] *Kyoto University, Kyoto 606-8502, Japan*
[x] *Laboratoire Leprince-Ringuet, Ecole Polytechnique, CNRS-IN2P3, Route de Saclay, F-91128, Palaiseau, France*
[y] *Lawrence Livermore National Laboratory, Livermore, CA 94550, United States*
[z] *Los Alamos National Laboratory, Los Alamos, NM 87545, United States*
[aa] *LPC, Université Blaise Pascal, CNRS-IN2P3, Clermont-Fd, 63177 Aubiere Cedex, France*
[ab] *Department of Physics, Lund University, Box 118, SE-221 00 Lund, Sweden*
[ac] *Institut für Kernphysik, University of Muenster, D-48149 Muenster, Germany*
[ad] *Myongji University, Yongin, Kyonggido 449-728, Republic of Korea*
[ae] *Nagasaki Institute of Applied Science, Nagasaki-shi, Nagasaki 851-0193, Japan*
[af] *University of New Mexico, Albuquerque, NM 87131, United States*
[ag] *New Mexico State University, Las Cruces, NM 88003, United States*
[ah] *Oak Ridge National Laboratory, Oak Ridge, TN 37831, United States*
[ai] *IPN-Orsay, Universite Paris Sud, CNRS-IN2P3, BP1, F-91406, Orsay, France*
[aj] *PNPI, Petersburg Nuclear Physics Institute, Gatchina, Leningrad region 188300, Russia*
[ak] *RIKEN Nishina Center for Accelerator-Based Science, Wako, Saitama 351-0198, Japan*
[al] *RIKEN BNL Research Center, Brookhaven National Laboratory, Upton, NY 11973-5000, United States*
[am] *Physics Department, Rikkyo University, 3-34-1 Nishi-Ikebukuro, Toshima, Tokyo 171-8501, Japan*
[an] *Saint Petersburg State Polytechnic University, St. Petersburg, Russia*
[ao] *Universidade de São Paulo, Instituto de Física, Caixa Postal 66318, São Paulo CEP05315-970, Brazil*
[ap] *System Electronics Laboratory, Seoul National University, Seoul, Republic of Korea*
[aq] *Chemistry Department, Stony Brook University, Stony Brook, SUNY, NY 11794-3400, United States*
[ar] *Department of Physics and Astronomy, Stony Brook University, SUNY, Stony Brook, NY 11794, United States*
[as] *SUBATECH (Ecole des Mines de Nantes, CNRS-IN2P3, Université de Nantes) BP 20722-44307, Nantes, France*
[at] *University of Tennessee, Knoxville, TN 37996, United States*
[au] *Department of Physics, Tokyo Institute of Technology, Oh-okayama, Meguro, Tokyo 152-8551, Japan*
[av] *Institute of Physics, University of Tsukuba, Tsukuba, Ibaraki 305, Japan*
[aw] *Vanderbilt University, Nashville, TN 37235, United States*
[ax] *Waseda University, Advanced Research Institute for Science and Engineering, 17 Kikui-cho, Shinjuku-ku, Tokyo 162-0044, Japan*
[ay] *Weizmann Institute, Rehovot 76100, Israel*
[az] *Yonsei University, IPAP, Seoul 120-749, Republic of Korea*

ARTICLE INFO

Article history:
Received 11 March 2009
Received in revised form 9 July 2009
Accepted 29 July 2009
Available online 3 August 2009
Editor: V. Metag

ABSTRACT

We present the first measurement of photoproduction of J/ψ and of two-photon production of high-mass e^+e^- pairs in electromagnetic (or ultra-peripheral) nucleus–nucleus interactions, using Au + Au data at $\sqrt{s_{NN}} = 200$ GeV. The events are tagged with forward neutrons emitted following Coulomb excitation of one or both Au* nuclei. The event sample consists of 28 events with $m_{e^+e^-} > 2$ GeV/c^2 with zero like-sign background. The measured cross sections at midrapidity of $d\sigma/dy\,(J/\psi + Xn, y = 0) =$

PACS:
13.40.-f
13.60.-r
24.85.+p
25.20.-x
25.20.Lj
25.75.-q

$76 \pm 33(\text{stat}) \pm 11(\text{syst})$ μb and $d^2\sigma/dm\,dy\,(e^+e^- + Xn,\, y = 0) = 86 \pm 23(\text{stat}) \pm 16(\text{syst})$ μb/(GeV/c^2) for $m_{e^+e^-} \in [2.0, 2.8]$ GeV/c^2 have been compared and found to be consistent with models for photoproduction of J/ψ and QED based calculations of two-photon production of e^+e^- pairs.

1. Introduction

The idea to use the strong electromagnetic fields present in high-energy nucleus–nucleus collisions to study photoproduction at hadron colliders has attracted growing interest in recent years, see [1–3] for reviews. Electromagnetic interactions can be studied without background from hadronic processes in ultra-peripheral collisions (UPC) without nuclear overlap, i.e. impact parameters larger than the sum of the nuclear radii. This study focuses on the measurement of exclusively produced high-mass e^+e^- pairs at midrapidity in Au + Au collisions at $\sqrt{s_{NN}} = 200$ GeV, $\text{Au} + \text{Au} \to \text{Au} + \text{Au} + e^+e^-$. The results have been obtained with the PHENIX detector [4] at the BNL Relativistic Heavy Ion Collider (RHIC).

The electromagnetic field of a relativistic particle can be represented by a spectrum of equivalent photons. This is the Weizsäcker–Williams method of virtual quanta [5,6]. The number of photons in the spectrum is proportional to Z^2, where Z is the charge number of the particle, and the equivalent two-photon luminosity is thus proportional to Z^4. The strong dependence on Z favours the use of heavy ions for studying two-photon and photonuclear processes. The virtualities of the equivalent photons when the field couples coherently to the entire nucleus are restricted by the nuclear form factor to $Q^2 = (\omega^2/(c\gamma)^2 + q_\perp^2) \lesssim (\hbar/R_A)^2$. Here, ω and $q_\perp$ are the photon energy and transverse momentum, respectively, R_A is the nuclear radius and γ the Lorentz factor of the beam. At RHIC energies, $\gamma = 108$ and the maximum photon energy in the center-of-mass system is of the order of $\omega_{\max} \sim 3$ GeV corresponding to maximum photon–nucleon and two-photon center-of-mass energies of $W_{\gamma N}^{\max} \sim 34$ GeV and $W_{\gamma\gamma}^{\max} \sim 6$ GeV.

The exclusive production of an e^+e^- pair can proceed either through a purely electromagnetic process (a two-photon interaction to leading order) or through coherent photonuclear production of a vector meson, which decays into an electron pair. Exclusive photoproduction of vector mesons is usually thought of as proceeding via Pomeron-exchange, the perturbative-QCD equivalent of which is the exchange of two gluons or a gluon ladder. The Feynman diagrams for the two leading order processes are shown in Fig. 1. The two-gluon picture is applicable to production of heavy vector mesons, such as the J/ψ, and to production of lighter mesons at high momentum transfers [7]. The J/ψ production cross section is consequently a good probe of the proton [8] and nuclear gluon distribution, $G_A(x, Q^2)$, as well as of vector-meson dynamics in nuclear matter [9,10]. For J/ψ-production, the coverage of the PHENIX central tracking arm, $-0.35 < \eta < 0.35$ corresponds to a range in the photon–nucleon center-of-mass energy between $21 < W_{\gamma N} < 30$ GeV, with a mean $\langle W_{\gamma N} \rangle = 24$ GeV. This corresponds to photon energies in the rest frame of the target nucleus of $240 < E_\gamma < 480$ GeV, with $\langle E_\gamma \rangle = 300$ GeV. Mid-rapidity photoproduction of J/ψ probes nuclear Bjorken-x values of $x = m_{J/\psi}^2/W_{\gamma A}^2 \approx 1.5 \times 10^{-2}$ [10], where the nuclear gluon density is partially depleted by "shadowing" effects [11] compared to the proton.

The strong fields associated with heavy ions at high energies lead to large probabilities for exchanging additional soft photons in the same event. Most of these photons have too low energy to produce particles, but they can excite the interacting nuclei. The dominating excitation is to a Giant-Dipole Resonance (GDR) with energies $\mathcal{O}(10$ MeV), which decays by emitting neutrons at very forward rapidities, providing a very useful means to trigger on UPCs with Zero-Degree Calorimeters (ZDC). The probability for having a Coulomb excitation leading to emission of neutrons in at least one direction in coincidence with coherent J/ψ production is $55\% \pm 6\%$ [12]. The probabilities for exchanging one or several photons factorise, i.e. the Coulomb tagging does not introduce any bias in the extraction of exclusive J/ψ photoproduction cross sections from these events [13]. The soft photons leading to moderate nuclear excitation are indicated to the right of the dashed line in Fig. 1. Incoherent (or quasi-elastic) vector-meson photoproduction can also proceed via the interaction of the exchanged photon with a *single* nucleon in the nucleus. In that case, J/ψ photoproduction is always accompanied by nuclear breakup and emission of nucleons in the forward direction [14].

Photoproduction of vector mesons has been studied with lepton beams first in the 60s [15,16] and more recently at the electron–proton collider HERA [17,18]. Measurements of photonuclear production of ρ mesons [19,20], as well as of two-photon production of *low-mass* e^+e^- pairs [21] in heavy ion interactions have been performed by the STAR Collaboration. The CDF Collaboration has studied two-photon production of e^+e^- pairs [22] and exclusive production of $\mu^+\mu^-$ pairs [23] in $p\bar{p}$ collisions at the Tevatron. The PHENIX analysis presented here is the first on heavy final states in ultra-peripheral nucleus–nucleus collisions. It supersedes a preliminary study presented earlier [24]. The cross section for J/ψ and e^+e^- photoproduction are compared with various theoretical calculations [10,14,25–27].

2. Experimental setup

The data presented here were collected with the PHENIX detector at RHIC during the 2004 high-luminosity Au + Au run at $\sqrt{s_{NN}} = 200$ GeV. The PHENIX detector [4], is a versatile detector designed to study the properties of strongly interacting matter at extreme temperatures and energy densities present in central heavy ion collisions. The current analysis demonstrates its capabilities to also study ultra-peripheral collisions, which have a very different event topology. The PHENIX central tracking system [28] consists of two arms, each covering $|\eta| < 0.35$ and $\Delta\phi = \pi/2$, equipped with multi-layer drift chambers (DC) followed by multi-wire proportional chambers (PC) with pixel-pad readout. The tracking arms also have Ring-Imaging-Čerenkov (RICH, with CO_2 gas radiator) detectors [29] and electromagnetic calorimeters (EMCal) [30] for electron and positron identification. The PHENIX EMCal consists of six sectors of lead-scintillator sandwich calorimeter (PbSc, 15552 individual towers with 5.54 cm × 5.54 cm × 37.5 cm,

* Corresponding author.
E-mail addresses: jacak@skipper.physics.sunysb.edu (B.V. Jacak), brant@bnl.gov (B.M. Johnson).
[1] Deceased.
[2] PHENIX Spokesperson.

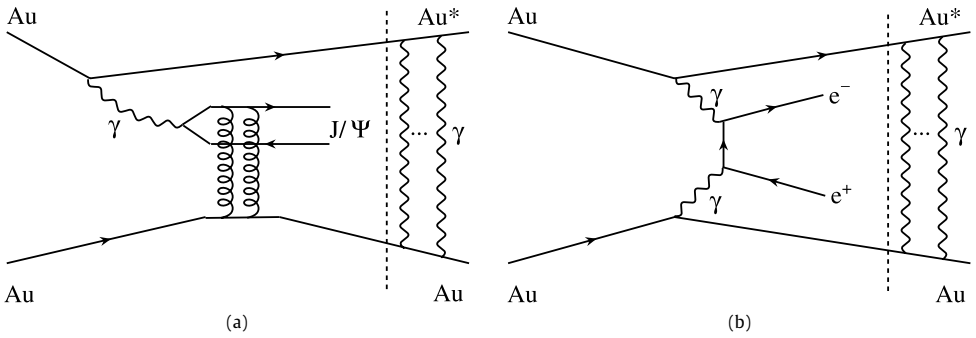

Fig. 1. Lowest order Feynman diagrams for exclusive photoproduction of (a) J/ψ and (b) dielectrons, in ultra-peripheral Au + Au collisions. The photons to the right of the dashed line are soft photons that may excite the nuclei but do not lead to particle production in the central rapidity region. Both diagrams contain at least one photon and occur when the nuclei are separated by impact parameters larger than the sum of the nuclear radii.

$18X_0$) and two sectors of lead-glass Čerenkov calorimeter (PbGl, 9216 modules with 4 cm × 4 cm × 40 cm, $14.4X_0$), at a radial distance of ∼ 5 m from the beam line.

The ultra-peripheral Au + Au events were tagged by neutron detection at small forward angles in the ZDC. The ZDCs [31,32] are hadronic calorimeters placed 18 m up- and down-stream of the interaction point that measure the energy of the neutrons coming from the Au* Coulomb dissociation with ∼ 20% energy resolution and cover $|\theta| < 2$ mrad, which is a very forward region.[3]

The events used in this analysis were collected with the UPC trigger set up for the first time in PHENIX during the 2004 run with the following characteristics:

(1) A veto on coincident signals in both Beam–Beam Counters (BBC, covering $3.0 < |\eta| < 3.9$ and full azimuth) selects exclusive-type events characterised by a large rapidity gap on either side of the central arm.
(2) The EMCal-Trigger (ERT) with a 2×2 tile threshold at 0.8 GeV. The trigger is set if the analog sum of the energy deposit in a 2×2 tile of calorimeter towers is above threshold (0.8 GeV).
(3) At least 30 GeV energy deposited in one or both of the ZDCs is required to select Au + Au events with forward neutron emission (Xn) from the (single or double) Au* decay.

The BBC trigger efficiency for hadronic Au + Au collisions is $92 \pm 3\%$ [33]. A veto on the BBC trigger has an inefficiency of 8%, which implies that the most peripheral nuclear reactions could be a potential background for our UPC measurement if they happen to have an electron pair in the final state. An extrapolation of the measured p–p dielectron rate [34] at $m_{\rm inv} > 2$ GeV/c^2 to the 8% most peripheral interactions – scaled by the corresponding number of nucleon–nucleon collisions (1.6) – results in a negligible contribution (only 0.4 e^+e^- pairs). On the other hand, the ERT trigger requirement (2) has an efficiency of 90 ± 10%, and the requirement (3) of minimum ZDC energy deposit(s) leaves about 55% of the coherent and about 100% of the incoherent J/psi events, as discussed above. All these trigger efficiencies and their uncertainties are used in the final determination of the production cross sections below.

The total number of events collected by the UPC trigger was 8.5 M, of which 6.7 M satisfied standard data quality assurance criteria. The useable event sample corresponds to an integrated luminosity $\mathcal{L}_{\rm int} = 141 \pm 12\ \mu{\rm b}^{-1}$ computed from the minimum bias triggered events.

[3] Much larger than the crossing angle of Au beams at the PHENIX interaction point (0.2 mrad).

3. Data analysis

Charged particle tracking in the PHENIX central arms is based on a combinatorial Hough transform in the track bend plane (perpendicular to the beam direction). The polar angle is determined from the position of the track in the PC outside the DC and the reconstructed position of the collision vertex [35]. For central collisions, the collision vertex is reconstructed from timing information from the BBC and/or ZDC. This does not work for UPC events, which, by definition, do not have BBC coincidences and often do not have ZDC coincidences. The event vertex was instead reconstructed from the position of the PC hits and EMCal clusters associated with the tracks in the event. This gave an event vertex resolution in the longitudinal direction of 1 cm. Track momenta are measured with a resolution $\delta p/p \approx 0.7\% \oplus 1.0\% p[{\rm GeV}/c]$ in minimum bias Au + Au nuclear collisions [36]. Only a negligible reduction in the resolution is expected in this analysis because of the different vertex resolution.

The following global cuts were applied to enhance the sample of genuine γ-induced events:

(1) A standard offline vertex cut $|vtx_z| < 30$ cm was required to select collisions well centered in the fiducial area of the central detectors and to avoid tracks close to the magnet poles.
(2) Only events with two charged particles were analyzed. This is a restrictive criterion imposed to cleanly select "exclusive" processes characterised by only two isolated particles (electrons) in the final state. It allows to suppress the contamination of non-UPC (mainly beam–gas and peripheral nuclear) reactions that fired the UPC trigger, whereas the signal loss is small (less than 5%).

Unlike the $J/\psi \to e^+e^-$ analyses in nuclear Au + Au reactions [36,37] which have to deal with large particle multiplicities, we did not need to apply very strict electron identification cuts in the clean UPC environment. Instead, the following RICH- and EMCal-based offline cuts were used:

(1) RICH multiplicity $n_0 \geqslant 2$ selects $e^\pm$ which fire 2 or more tubes around the track within the nominal ring radius.
(2) Candidate tracks with an associated EMCal cluster with dead or noisy towers within a 2 × 2 tile are excluded.
(3) At least one of the tracks in the pair is required to pass an EMCal cluster energy cut ($E_1 > 1$ GeV ∥ $E_2 > 1$ GeV) to select candidate $e^\pm$ in the plateau region above the turn-on curve of the ERT trigger (which has a 0.8 GeV threshold).

Beyond those global or single-track cuts, an additional "coherent" identification cut was applied by selecting only those e^+e^- candi-

dates detected in opposite arms. Such a cut aims at reducing the high-p_T pairs while improving the detection of the low-p_T pairs expected for $\gamma\gamma$, γA production. Nevertheless, after all the previous cuts were applied the influence of this selection is found to be small; there is only one event in which the e^+ and e^- are in the same arm and have $m_{e^+e^-} > 2$ GeV/c^2.

Finally, J/ψ were reconstructed by invariant mass analysis of the measured e^+e^- pairs. There was no remaining like-sign background after the aforementioned analysis cuts.

The cross sections were obtained after correcting the raw number of signal counts for the geometrical acceptance of our detector system, and the efficiency losses introduced by the previously described analysis cuts. Acceptance and efficiency corrections were obtained using the PHENIX GEANT3 [38] simulation package with input distributions from the STARLIGHT Monte Carlo (MC), based on the models presented in [12,25,39]. The measured $\gamma + p \to V + p$ cross sections from HERA and fixed target experiments with lepton beams are used as input to the models. STARLIGHT well reproduces the existing $d^3N/dy\,d\phi\,dp_T$ distribution of coherent ρ production in UPC Au + Au events measured at RHIC by STAR [19,20]. Helicity conservation is assumed in the model, and the angular distribution of the decay products ($J/\psi \to e^+e^-$) is given by $dN/d\cos(\theta) \propto 1 + \cos^2(\theta)$ in the J/ψ center-of-mass. The angular distribution is different from that for ρ production followed by the decay $\rho \to \pi^+\pi^-$, because of the different spin of the daughters, as well as from the angular distribution in two-photon interactions $\gamma + \gamma \to e^+e^-$. We generated 5×10^4 coherent J/ψ and 8×10^6 coherent high-mass e^+e^- pairs ($m_{e^+e^-} > 1$ GeV/c^2) in Au+Au collisions accompanied by forward neutron emission. The simulated events were passed through the same reconstruction programme as the real data.

Table 1
Coherent J/ψ and e^+e^- (continuum) acceptance and efficiency for $|y_{pair}| < 0.35$ as a function of invariant mass range. The last line shows the trigger efficiency.

$m_{e^+e^-}$ [GeV/c^2]	$Acc \times \varepsilon$
J/ψ	$(2.49 \pm 0.25) \times 10^{-2}$
e^+e^- [2.0, 2.8]	$(2.24 \pm 0.22) \times 10^{-3}$
e^+e^- [2.0, 2.3]	$(2.16 \pm 0.22) \times 10^{-3}$
e^+e^- [2.3, 2.8]	$(2.33 \pm 0.23) \times 10^{-3}$
ϵ_{trigg}	0.9 ± 0.1

Table 1 summarises the J/ψ and dielectron acceptance and efficiency correction factors obtained from our simulation studies. For instance, for J/ψ photoproduction the correction is $1/(2.49 \pm 0.25)$%, of which the experimental acceptance to detect the decay electron pair is about 5% (for J/ψ produced at $|y| < 0.35$). In the $\gamma\gamma \to e^+e^-$ sample, most of the electrons/positrons are emitted at very forward angles. The fraction of events with $|y_{pair}| < 0.35$ and $2.0 < m_{e^+e^-} < 2.8$ GeV/c^2, where both the electron and positron are within $|\eta| < 0.35$ is 1.10%. The corresponding numbers for $2.0 < m_{e^+e^-} < 2.3$ GeV/c^2 and $2.3 < m_{e^+e^-} < 2.8$ GeV/c^2 are 1.11% and 1.08%, respectively. The acceptance and efficiency corrections have a systematic uncertainty of 10% resulting from the accuracy of the simulation to describe the detector, the electron identification parameters, and the event vertex position resolution.

4. Results and discussion

The measured e^+e^- invariant mass distribution for the sample is shown in Fig. 2(a). The amount of background can be estimated from the number of like-sign events (i.e. events where two electrons or two positrons are reconstructed). We find no like-sign pairs for $m_{e^\pm e^\pm} > 2$ GeV/c^2, compared with 28 events with an e^+e^- pair with $m_{e^+e^-} > 2$ GeV/c^2. The shape is consistent with the expected contribution from the two processes in Fig. 1: a continuum distribution corresponding to two-photon production of e^+e^- pairs and a contribution from $J/\psi \to e^+e^-$. Since the offline cuts ($E_1 > 1$ GeV $\parallel$ $E_2 > 1$ GeV) cause a sharp drop in the efficiency for $m_{e^+e^-} < 2$ GeV/c^2, we include only pairs with $m_{e^+e^-} \geqslant 2$ GeV/c^2 in the analysis.

The invariant mass distribution is fitted with a continuum (exponential) curve combined with a Gaussian function at the J/ψ peak, as shown by the solid curve in Fig. 2(a). Simulations based on events generated by the STARLIGHT MC (see last paragraphs of Section 3) processed through GEANT have shown that the shape of the measured continuum contribution is well described by an exponential function $dN/dm_{e^+e^-} = A \cdot e^{cm_{e^+e^-}}$. Those simulations allow us to fix the exponential slope parameter to $c = -1.9 \pm 0.1$ GeV^{-1} c^2. The combined data fit is done with three free parameters: the exponential normalisation (A), the J/ψ yield and the J/ψ peak width (the Gaussian peak position has been fixed at the known J/ψ mass of $m_{J/\psi} = 3.097$ GeV/c^2 [40]). Fig. 2(b) shows the resulting invariant mass distribution obtained by subtracting the fitted exponential curve of the dielectron continuum from the

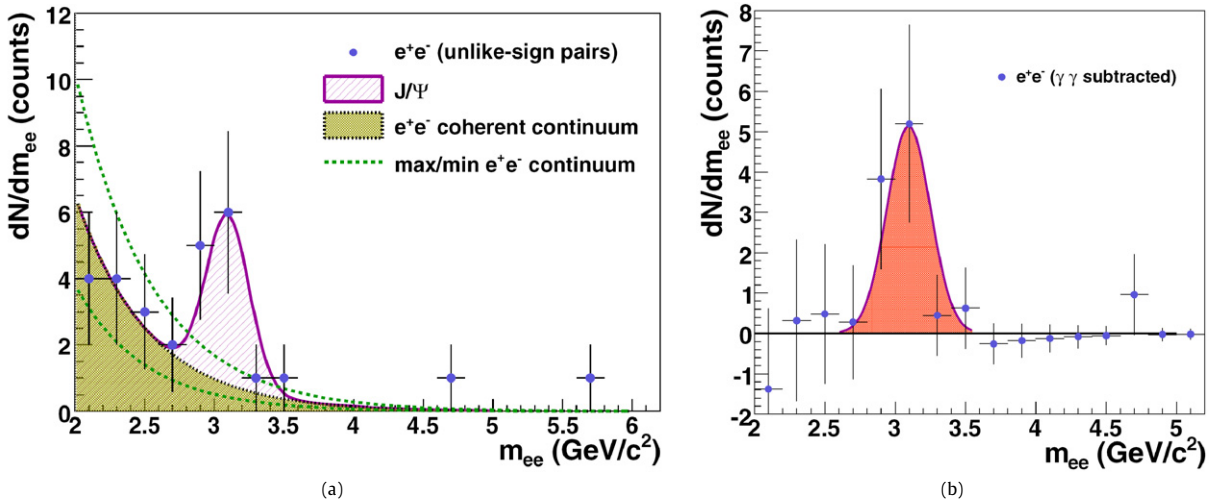

(a) (b)

Fig. 2. Left: (a) Invariant mass distribution of e^+e^- pairs fitted to the combination of (shaded) a dielectron continuum [exponential distribution] and (hatched) a J/ψ [Gaussian] signal. The two additional dashed curves indicate the maximum and minimum continuum contributions considered in this analysis (see text). (b) J/ψ invariant mass distribution after subtracting the fitted dielectron continuum signal in (a).

total experimental e^+e^- pairs distribution. There is a clear J/ψ peak, the width of which ($\sigma_{J/\psi} \sim 155$ MeV/c^2) is consistent with the J/ψ width from our full MC.

The J/ψ and continuum yields and the corresponding statistical errors are calculated from the fit. The dashed curves in Fig. 2(a) show the maximum and minimum e^+e^- continuum contributions considered, including both the statistical and systematical uncertainties. The systematic uncertainties were determined varying the dielectron continuum subtraction method using a power-law form instead of an exponential function and by modifying the corresponding fitted slope parameters by $\pm 3\sigma$. The propagated uncertainty of the extracted yields was estimated to be one count in both cases. The total number of J/ψ's is: $N_{J/\psi} = 9.9 \pm 4.1(\text{stat}) \pm 1.0(\text{syst})$, and the number of e^+e^- continuum pairs for $m_{e^+e^-} \in [2.0, 2.8]$ GeV/c^2 is: $N_{e^+e^-} = 13.7 \pm 3.7(\text{stat}) \pm 1.0(\text{syst})$. Table 2 shows the obtained results per invariant mass range.

Table 2
$J/\psi \to e^+e^-$ and e^+e^- continuum yields obtained from the fit of the data to an exponential plus Gaussian function per invariant mass range. Systematic errors are obtained as described in the text.

$m_{e^+e^-}$ [GeV/c^2]	Yield
J/ψ	$N_{J/\psi} = 9.9 \pm 4.1(\text{stat}) \pm 1.0(\text{syst})$
e^+e^- [2.0, 2.8]	$N_{e^+e^-} = 13.7 \pm 3.7(\text{stat}) \pm 1.0(\text{syst})$
e^+e^- [2.0, 2.3]	$N_{e^+e^-} = 7.4 \pm 2.7(\text{stat}) \pm 1.0(\text{syst})$
e^+e^- [2.3, 2.8]	$N_{e^+e^-} = 6.2 \pm 2.5(\text{stat}) \pm 1.0(\text{syst})$

Fig. 3(a) shows a scatter plot of invariant mass $m_{e^+e^-}$ vs. pair p_T. From the plot, it is clear that most of the pairs outside the J/ψ peak originate in coherent processes with very low pair transverse momenta ($p_T \lesssim 100$ MeV/c), as expected for two-photon interactions. For events with $m_{e^+e^-}$ around the J/ψ mass, however, there are a few counts at larger p_T values which can be ascribed neither to the experimental p_T resolution nor to background events, since there are no like-sign pairs above 2 GeV/c^2. A purely coherent production – corresponding to events where the fields couple coherently to all nucleons and the nucleus remains in its ground state ($\gamma + A \to V + A$) – would yield $p_T \lesssim 200$ MeV/c after reconstruction. On the other hand, incoherent production ($\gamma + A \to V + X$) – dominated by the quasi-elastic vector meson production off one nucleon inside the nucleus, $\gamma + N \to V + N$ – results in much larger p_T for the photoproduced J/ψ [14]. The cross sections for coherent and incoherent J/ψ photoproduction in UPCs at RHIC are expected to be of the same order [14]. We discuss below whether our data confirm such a prediction.

The transverse momentum distribution of the events with $m_{e^+e^-} > 2$ GeV/c^2 is shown in Fig. 3(b). For clarity, only points below $p_T < 1$ GeV/c are drawn. The p_T is here the magnitude of the vector sum of the $\vec{p_T}$ of the electron and positron. One sees a

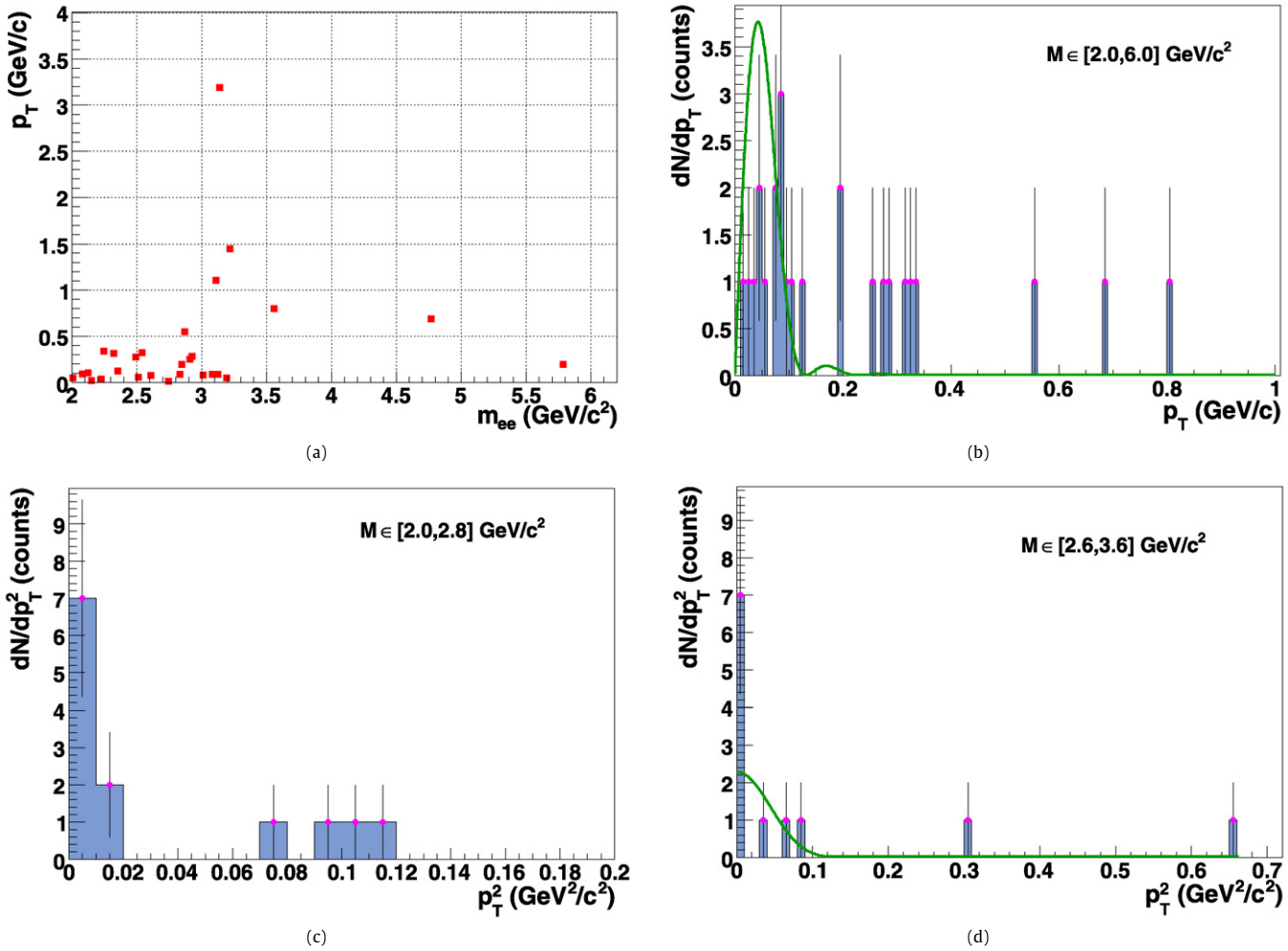

Fig. 3. Top: (a) Scatter plot of $e^+e^- m_{e^+e^-}$ vs. pair p_T. (b) dN/dp_T distribution of the pairs with $m_{e^+e^-} \in [2.0, 6.0]$ GeV/c^2 compared to the Au nuclear form factor, Eq. (1), and for simplicity showing only points with $p_T < 1$ GeV/c. Bottom: dN/dp_T^2 distributions of pairs with (c) $m_{e^+e^-} \in [2.0, 2.8]$ GeV/c^2 and (d) $m_{e^+e^-} \in [2.6, 3.6]$ GeV/c^2 compared to the expected Au nuclear form factor, also for clarity only points with $p_T^2 < 0.7$ GeV^2/c^2 are drawn. Note the difference in scale on the x-axis in the four plots.

Table 3
Measured J/ψ and e^+e^- continuum photoproduction cross sections at midrapidity in ultra-peripheral Au + Au collisions (accompanied with forward neutron emission) at $\sqrt{s_{NN}} = 200$ GeV. The rightmost column in the lower part shows the STARLIGHT predictions [39].

J/ψ	$d\sigma/dy\|_{y=0}$ [μb] $76 \pm 31(\text{stat}) \pm 15(\text{syst})$	
$m_{e^+e^-}$ [GeV/c^2]	$d^2\sigma/dm_{e^+e^-}\,dy\|_{y=0}$ [μb/(GeV/c^2)] data	STARLIGHT
e^+e^- continuum [2.0, 2.8]	$86 \pm 23(\text{stat}) \pm 16(\text{syst})$	90
e^+e^- continuum [2.0, 2.3]	$129 \pm 47(\text{stat}) \pm 28(\text{syst})$	138
e^+e^- continuum [2.3, 2.8]	$60 \pm 24(\text{stat}) \pm 14(\text{syst})$	61

clear enhancement of events with very low transverse momenta, consistent with coherent production. The squared form-factor of a gold nucleus,

$$\left|F_{\text{Au}}\left(p_{\text{T}}^2\right)\right|^2 = \left|3\frac{\sin(Rp_{\text{T}}) - Rp_{\text{T}}\cos(Rp_{\text{T}})}{(Rp_{\text{T}})^3(1+(ap_{\text{T}})^2)}\right|^2, \tag{1}$$

is shown for comparison. Here, $R = 6.7$ fm is the gold radius, and $a = 0.7$ fm represents the diffuseness of the nuclear surface [41]. The magnitude of the form-factor is a free parameter fitted to reproduce the spectra. Fig. 3 also presents the corresponding distribution expressed in terms of the squared momentum transfer from the target nucleus, $p_{\text{T}}^2 \approx -t$, for events with $m_{e^+e^-}$ corresponding to the dielectron continuum $m_{e^+e^-} \in [2.0, 2.8]$ GeV/c^2 (Fig. 3(c) and below the J/ψ-peak, $m_{e^+e^-} \in [2.6, 3.6]$ GeV/c^2 (Fig. 3(d)). The 4 events with $p_T^2 \approx 0.1$ GeV/c^2 in Fig. 3(c) have transverse momenta slightly above what one would expect for two-photon production. They could thus be due to some other, incoherent production process for dielectron pairs. The simulations of the experimental resolution show, however, that a spread in p_T of that magnitude can also be caused by the experimental resolution. We therefore include also these events in the calculation of the continuum cross section.

The extracted yields of J/ψ and e^+e^- are used to calculate the final cross section for photoproduction at midrapidity in ultra-peripheral Au + Au collisions accompanied by forward neutron emission. For dielectrons at midrapidity (y is the rapidity of the pair) the double differential cross section is:

$$\begin{aligned}\frac{d^2\sigma_{e^+e^-+Xn}}{dy\,dm_{e^+e^-}} &= \frac{N_{e^+e^-}}{Acc\cdot\varepsilon\cdot\varepsilon_{\text{trigg}}\cdot\mathcal{L}_{\text{int}}}\cdot\frac{1}{\Delta y}\cdot\frac{1}{\Delta m_{e^+e^-}} \\ &= 86 \pm 23(\text{stat}) \pm 16(\text{syst})\ \mu\text{b}/\left(\text{GeV}/c^2\right) \\ &\quad \text{for } m_{e^+e^-} \in [2.0, 2.8]\ \text{GeV}/c^2 \text{ and } |y| < 0.35. \end{aligned} \tag{2}$$

For J/ψ at midrapidity ($|y| < 0.35$) the differential cross section is:

$$\begin{aligned}\frac{d\sigma_{J/\psi+Xn}}{dy} &= \frac{1}{\text{BR}}\cdot\frac{N_{J/\psi}}{Acc\cdot\varepsilon\cdot\varepsilon_{\text{trigg}}\cdot\mathcal{L}_{\text{int}}}\cdot\frac{1}{\Delta y} \\ &= 76 \pm 31(\text{stat}) \pm 15(\text{syst})\ \mu\text{b}. \end{aligned} \tag{3}$$

The correction factors (and corresponding uncertainties) are quoted in Table 1 as described in previous sections, and BR = 5.94% is the known J/ψ dielectron branching ratio [40]. Table 3 summarises the measured cross sections per invariant mass interval.

The measured dielectron cross sections at midrapidity are in very good agreement with the STARLIGHT predictions for coherent dielectron photoproduction (rightmost column of Table 3) [39]. Exclusive dilepton production in STARLIGHT is calculated combining the two equivalent (Weizsäcker–Williams) photon fluxes from each ion with the Breit–Wheeler formula for $\gamma\gamma \to l^+l^-$. The agreement between STARLIGHT and other leading order calculations [42] is good as long as the pair invariant mass is not too low. A recent calculation has found that higher order terms suppress the e^+e^- cross section by 29% in the invariant mass range $140 < m_{e^+e^-} < 165$ MeV/c^2 [43]. A reduction of the same magnitude in the invariant mass range considered here, $2.0 < m_{e^+e^-} < 2.8$ GeV/c^2, would still be in agreement with our measurement.

The final $J/\psi + Xn$ cross section is compared to the theoretical predictions computed in references [12,14,25,27,39,44] in Fig. 4. The rapidity distributions for the coherent production of Strikman et al. [14] and Ivanov et al. [27] have been scaled down according to [12] to account for the reduction of the yield expected when requiring coincident forward neutron emission (Xn). The scaling has been applied as a function of rapidity with the integrated cross section being 55% of the original one.

The upper limit of the band covered by the Strikman et al. predictions corresponds to calculations in the impulse approximation (no shadowing), and the lower limit corresponds to calculations using the eikonal (Glauber) model with $\sigma(J/\Psi + N) = 3$ mb. The bands for the calculations of Ivanov et al. corresponds to two different parameterisations of the dipole cross section [27]. The predictions by [14] and [27] for the coherent and incoherent photoproduction cross sections are drawn separately in Fig. 4(a) and summed up in Fig. 4(b). STARLIGHT [12,25,39] and Gonçalves–Machado [44] calculations only evaluate the coherent contribution.

As mentioned above, the measured pair p_{T} distributions suggest coherent J/ψ photoproduction ($\gamma + A \to J/\psi + X$) and a possible additional incoherent ($\gamma + N \to J/\psi + X$) contribution at higher p_{T}. To give an indicative estimate of the size of the incoherent contribution, we can assume that it corresponds to the counts in the J/ψ mass window with $p_{\text{T}}^2 > 0.1(0.05)$ GeV$^2/c^2$. This corresponds to about 4(6) counts, which amounts to a contribution of about 40(60)% of the total J/ψ production, compatible with the theoretical calculations [14]. The limited data statistics prevents us from separating in a more quantitative way the two components. Note that although the acceptance correction for the J/ψ was calculated using a Monte Carlo which includes only the coherent component, the obtained correction is also a reasonable approximation for the incoherent component, provided that quasi-elastic scattering on a single nucleon, $\gamma + N \to V + N$, gives the main contribution. The polarisation of the vector meson will then be the same as for coherent production, and the reduction in acceptance because of the different p_{T} range will be of the order of ~ 10–20%. If the incoherent contribution to the total J/ψ photoproduction was 40%, the coherent J/ψ cross section would become ~ 46 μb.

Despite these uncertainties, the final J/ψ cross section is in good agreement, within the (still large) statistical errors, with the theoretical values computed in [12,14,25,27,39,44] as shown in Fig. 4. The current uncertainties unfortunately preclude any more detailed conclusion at this point regarding the two crucial ingredients of the models (nuclear gluon shadowing and J/ψ nuclear absorption cross section). The statistical uncertainties can be improved with significantly higher Au + Au luminosities and a concurrent measurement of the J/ψ in the dimuon decay channel in the more forward acceptances covered by the PHENIX muon spectrometers.

Finally, one can attempt to compare the obtained photonuclear J/ψ cross sections to those from e–p collisions at HERA by dividing the measured differential cross section ($d\sigma/dy$) with the (theoretical) equivalent photon spectrum ($dN_\gamma/d\omega$). At midrapidity: $\sigma_{\gamma A\to J/\psi A} = (d\sigma_{AA\to J/\psi AA}/dy)/(2\,dN_\gamma/d\omega)$, with $2\,dN_\gamma/d\omega = 6.7$ (10.5) for the coherent (incoherent) spectrum at a photon–nucleon center-of-mass energy of $\langle W_{\gamma p}\rangle = 24$ GeV [12]. Assuming, for the sake of simplicity, a 50%–50% contribution from coherent and in-

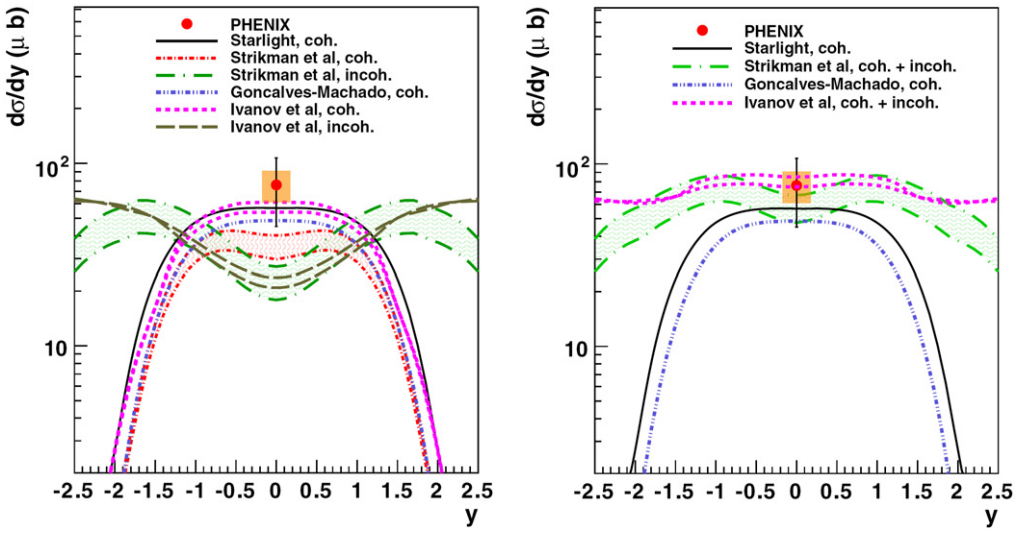

Fig. 4. Measured cross section of $J/\psi + Xn$ production at midrapidity in UPC Au + Au collisions at $\sqrt{s_{NN}} = 200$ GeV. The error bars (boxes) show the statistical (systematical) uncertainties. When available, the theoretical calculations for the coherent and incoherent components are shown separately in (a), and summed up in (b). The theoretical calculations (a) in order from top to bottom near $y = 0$: (short dashed lines) coherent Ivanov et al. [27], (solid line) coherent STARLIGHT [12,25,39], (dashed-double-dotted line) Goncalves–Machado [44], (shaded between short dashed-dotted lines) coherent Strikman et al. [14], (shaded between long dashed-dotted dashed lines) incoherent Strikman et al. [14], and (long dashed lines) coherent Ivanov et al. [27]. And (b) in order from top to bottom near $y = 0$: (short dashed lines) Ivanov et al. [27], (shaded between long dashed-dotted solid lines) Strikman et al. [14], (solid line) STARLIGHT [12,25,39], and (dashed–double-dotted line) Goncalves–Machado [44].

coherent interactions in our total ultra-peripheral J/ψ sample, the extracted photonuclear cross sections are: $\sigma(\gamma + \mathrm{Au} \to J/\psi + \mathrm{Au}) = 5.7 \pm 2.3(\mathrm{stat}) \pm 1.2(\mathrm{syst})$ μb, and $\sigma(\gamma + \mathrm{Au} \to J/\psi + X) = 3.6 \pm 1.4(\mathrm{stat}) \pm 0.7(\mathrm{syst})$ μb, respectively. A fit to the results from the H1 and ZEUS Collaborations [17,18] over their measured energy range gives $\sigma(\gamma + p \to J/\psi + p) = 30.5 \pm 2.7$ nb at $W_{\gamma p} = 24$ GeV. Therefore, the ratios $\sigma(\gamma + \mathrm{Au} \to J/\psi)/\sigma(\gamma + p \to J/\psi) = 186 \pm 88$, 118 ± 54 for the coherent and incoherent components (statistical and systematic errors assumed independent and added in quadrature) are consistent with a scaling of the photonuclear cross section with the number of nucleons in gold ($A = 179$): $\sigma(\gamma + \mathrm{Au} \to J/\psi) = A^{\alpha}\, \sigma(\gamma + p \to J/\psi)$ with $\alpha_{\mathrm{coh}} = 1.01 \pm 0.07$, and $\alpha_{\mathrm{incoh}} = 0.92 \pm 0.08$, respectively.[4]

5. Summary and conclusions

We have presented the first exclusive photoproduction of $J/\psi \to e^+e^-$ and high-mass e^+e^- pairs ever measured in nucleus–nucleus (as well as hadron–hadron) interactions. The measurement has been carried out by the PHENIX experiment in ultra-peripheral Au + Au interactions at $\sqrt{s_{NN}} = 200$ GeV tagged by forward (ZDC) neutron detection from the (single or double) Au* dissociation. Clear signals of J/ψ and high mass dielectron continuum have been found in the data. We have observed 28 e^+e^- pairs in $m_{e^+e^-} \in [2.0, 6.0]$ GeV/c^2 with zero like-sign background. Their p_{T} spectrum is peaked at low $p_{\mathrm{T}} \approx 90$ MeV/c as expected for coherent photoproduction with a realistic Au nuclear form factor.

The measured number of continuum e^+e^- events in the PHENIX acceptance for $m_{e^+e^-} \in [2.0, 2.8]$ GeV/c^2 is: $N(e^+e^-) = 13.7 \pm 3.7(\mathrm{stat}) \pm 1.0(\mathrm{syst})$. After correcting for acceptance and efficiency losses and normalising by the measured luminosity, we obtain a cross section of $d^2\sigma/dm_{e^+e^-}\, dy\, (e^+e^- + Xn)|_{y=0} = 86 \pm 23(\mathrm{stat}) \pm 16(\mathrm{syst})$ μb/(GeV/c^2), which is in good agreement with theoretical expectations for coherent exclusive dielectron production in photon–photon interactions.

The measured invariant mass distribution has a clear peak at the J/ψ mass with an experimental width in good agreement with a full GEANT-based simulation for UPC production and reconstruction in the PHENIX detector. The measured number of J/ψ mesons in the PHENIX acceptance is: $N(J/\psi) = 9.9 \pm 4.1(\mathrm{stat}) \pm 1.0(\mathrm{syst})$. The higher p_{T} distribution suggests an additional incoherent contribution to J/ψ photoproduction in accordance with predictions [14], but statistical limitations prevent a more quantitative estimate. After correcting for acceptance and efficiency losses and normalising by the measured luminosity, the total J/ψ photoproduction cross section is $d\sigma/dy\, (J/\psi + Xn)|_{y=0} = 76 \pm 31(\mathrm{stat}) \pm 15(\mathrm{syst})$ μb, which is consistent (within uncertainties) with theoretical expectations. The low background in the present data sample shows that future higher luminosity runs with reduced experimental uncertainties of the measured cross sections will provide more quantitative information on the nuclear gluon distribution and J/ψ absorption in cold nuclear matter at RHIC energies.

Acknowledgements

We thank the staff of the Collider-Accelerator and Physics Departments at BNL for their vital contributions. We acknowledge support from the Office of Nuclear Physics in DOE Office of Science and NSF (USA), MEXT and JSPS (Japan), CNPq and FAPESP (Brazil), NSFC (China), IN2P3/CNRS, and CEA (France), BMBF, DAAD, and AvH (Germany), OTKA (Hungary), DAE (India), ISF (Israel), KRF and KOSEF (Korea), MES, RAS, and FAAE (Russia), VR and KAW (Sweden), US CRDF for the FSU, US–Hungarian NSF-OTKA-MTA, and US–Israel BSF.

References

[1] G. Baur, K. Hencken, D. Trautmann, S. Sadovsky, Y. Kharlov, Phys. Rep. 364 (2002) 359.
[2] C.A. Bertulani, S.R. Klein, J. Nystrand, Annu. Rev. Nucl. Part. Sci. 55 (2005) 271.
[3] A. Baltz, et al., Phys. Rep. 458 (2008) 1.

[4] Note, for comparison, that repeating the same exercise for the photoproduced ρ in the STAR UPC measurement [20], $\sigma(\gamma + \mathrm{Au} \to \rho + \mathrm{Au}) = 530 \pm 19(\mathrm{stat}) \pm 57(\mathrm{syst})$ μb for $\langle W_{\gamma N} \rangle \sim 12.5$ GeV, and taking the experimentally-derived value $\sigma(\gamma + p \to \rho + p) = 9.88$ μb from [25], yields $\alpha_{\mathrm{coh}} = 0.75 \pm 0.02$ closer to the $A^{2/3}$-scaling expected for soft particle production.

[4] K. Adcox, et al., PHENIX Collaboration, Nucl. Instrum. Methods A 499 (2003) 469.
[5] C.F. von Weizsacker, Z. Phys. 88 (1934) 612.
[6] E.J. Williams, Phys. Rev. 45 (1934) 729.
[7] S. Mohrdieck, et al., H1 Collaboration, hep-ex/0205054, 2002.
[8] M.G. Ryskin, R.G. Roberts, A.D. Martin, E.M. Levin, Z. Phys. C 76 (1997) 231.
[9] L. Frankfurt, W. Koepf, M. Strikman, Phys. Rev. D 54 (1996) 3194.
[10] L. Frankfurt, M. Strikman, M. Zhalov, Phys. Lett. B 540 (2002) 220.
[11] N. Armesto, J. Phys. G 32 (2006) R367.
[12] A.J. Baltz, S.R. Klein, J. Nystrand, Phys. Rev. Lett. 89 (2002) 012301; A.J. Baltz, S.R. Klein, J. Nystrand, private communication.
[13] G. Baur, K. Hencken, A. Aste, D. Trautmann, S.R. Klein, Nucl. Phys. A 729 (2003) 787.
[14] M. Strikman, M. Tverskoy, M. Zhalov, Phys. Lett. B 626 (2005) 72.
[15] L. Lanzerotti, et al., Phys. Rev. Lett. 15 (1965) 210.
[16] T.H. Bauer, R.D. Spital, D.R. Yennie, F.M. Pipkin, Rev. Mod. Phys. 50 (1978) 261.
[17] S. Chekanov, et al., ZEUS Collaboration, Eur. Phys. J. C 24 (2002) 345.
[18] A. Aktas, et al., H1 Collaboration, Eur. Phys. J. C 46 (2006) 585.
[19] C. Adler, et al., STAR Collaboration, Phys. Rev. Lett. 89 (2002) 272302.
[20] B.I. Abelev, et al., STAR Collaboration, Phys. Rev. C 77 (2008) 034910.
[21] J. Adams, et al., STAR Collaboration, Phys. Rev. C 70 (2004) 031902.
[22] A. Abulencia, et al., CDF Collaboration, Phys. Rev. Lett. 98 (2007) 112001.
[23] T. Aaltonen, et al., CDF Collaboration, Phys. Rev. Lett. 102 (2009) 242001.
[24] D. d'Enterria, et al., PHENIX Collaboration, nucl-ex/0601001.
[25] S. Klein, J. Nystrand, Phys. Rev. C 60 (1999) 014903.
[26] V.P. Goncalves, M.V.T. Machado, J. Phys. G 32 (2006) 295.
[27] Y.P. Ivanov, B.Z. Kopeliovich, I. Schmidt, arXiv:0706.1532 [hep-ph]; B. Kopeliovich, private communication.
[28] K. Adcox, et al., PHENIX Collaboration, Nucl. Instrum. Methods A 499 (2003) 489.
[29] M. Aizawa, et al., PHENIX Collaboration, Nucl. Instrum. Methods A 499 (2003) 508.
[30] L. Aphecetche, et al., PHENIX Collaboration, Nucl. Instrum. Methods A 499 (2003) 521.
[31] C. Adler, et al., Nucl. Instrum. Methods A 470 (2001) 488.
[32] M. Chiu, A. Denisov, E. Garcia, J. Katzy, S. White, Phys. Rev. Lett. 89 (2002) 012302.
[33] S.S. Adler, et al., PHENIX Collaboration, Phys. Rev. Lett. 91 (2003) 072301.
[34] A. Adare, et al., PHENIX Collaboration, Phys. Lett. B 670 (2009) 313.
[35] J.T. Mitchell, et al., PHENIX Collaboration, Nucl. Instrum. Methods A 482 (2002) 491.
[36] S.S. Adler, et al., PHENIX Collaboration, Phys. Rev. C 69 (2004) 014901.
[37] A. Adare, et al., PHENIX Collaboration, Phys. Rev. Lett. 98 (2007) 232301.
[38] GEANT 3.2.1, CERN program library (1993).
[39] J. Nystrand, Nucl. Phys. A 752 (2005) 470.
[40] C. Amsler, et al., Phys. Lett. B 667 (2008) 1.
[41] K.T.R. Davies, J.R. Nix, Phys. Rev. C 14 (1976) 1977.
[42] G. Baur, K. Hencken, D. Trautmann, Phys. Rep. 453 (2007) 1.
[43] A.J. Baltz, Phys. Rev. Lett. 100 (2008) 062302.
[44] V.P. Goncalves, M.V.T. Machado, arXiv:0706.2810 [hep-ph].